

chem 5390

Advanced X-ray Analysis



LECTURE 18b

Dr. Teresa D. Golden
University of North Texas
Department of Chemistry

Application of Diffraction Data

XRD can be used for:

- Bravais lattice determination – phase determination (crystalline phases and orientation)
- Lattice parameter determination
- Determination of solvus line in phase diagrams (order-disorder transformation)
- Long range order
- Crystallite size and Strain
- Temperature factor – thermal diffuse scattering (thermal expansion)
- Thickness measurements of thin films and multilayers

Application of Diffraction Data

XRD can be used for:

- Bravais lattice determination – phase determination (crystalline phases and orientation)
- Lattice parameter determination
- Determination of solvus line in phase diagrams (order-disorder transformation)
- Long range order (Texture Analysis)
- Crystallite size and Strain**
- Temperature factor – thermal diffuse scattering (thermal expansion)
- Thickness measurements of thin films and multilayers

Application of Diffraction Data

Several other factors can contribute to peak broadening.

- Instrumental Peak Profile
- Crystallite Size
- **Microstrain**
 - Non-uniform Lattice Distortions
 - Faulting
 - Dislocations
 - Antiphase Domain Boundaries
 - Grain Surface Relaxation
- **Macrostrain**
- Solid Solution Inhomogeneity
- Temperature Factors

Application of Diffraction Data

Non-Uniform Lattice Distortions

Macrostrain when stress is uniformly compressive or tensile to cause the distance within the unit cell to become smaller or larger.

Causes the lattice parameters to change resulting in a peak shift.

Glycolation or heating of clay minerals are examples of induced macrostrains.

Application of Diffraction Data

Non-Uniform Lattice Distortions

Microstrain – produces a distribution of both tensile and compressive forces in the material. Results in a broadening of the diffraction peaks or peak asymmetry in some cases.

Dislocations, vacancies, shear planes, thermal expansion or contractions, etc can produce **Microstress**. The result can be a distribution of peaks around the unstressed peak location, appearing like a crude broadening of the peak.

Application of Diffraction Data

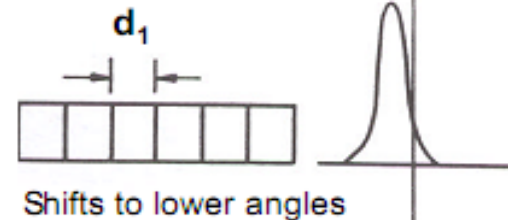
Effect of Lattice Strain on Diffraction Peak Position and Width

No Strain



Uniform Strain
 $(d_1 - d_0)/d_0$

Peak moves, no shape changes



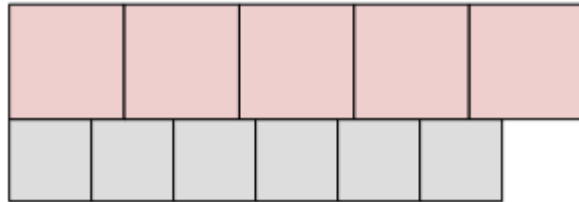
Non-uniform Strain
 $d_1 \neq \text{constant}$
Peak broadens



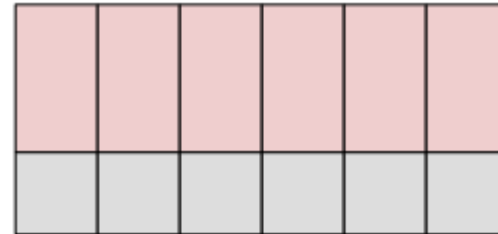
Exceeds d_0 on top, smaller than d_0 on the bottom
 $2\theta \rightarrow$

Application of Diffraction Data

Relaxation and Lattice Strain



Relaxed Film

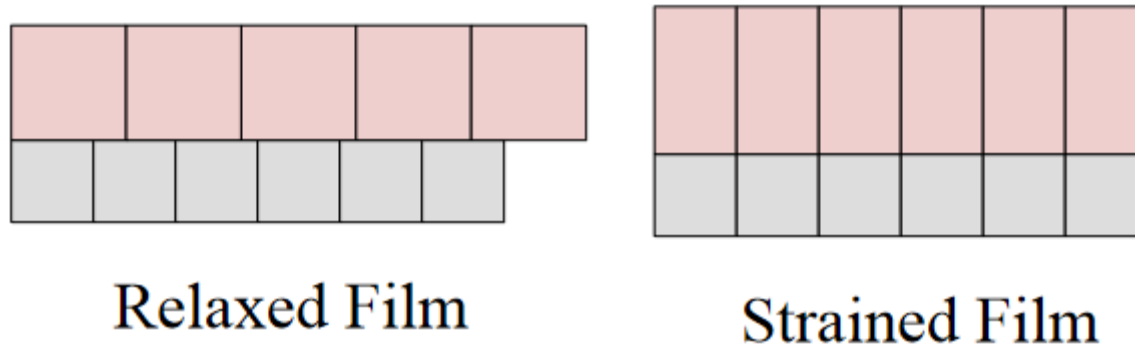


Strained Film

- If the film is mismatched to the substrate, then the film might be strained so that the lattice parameters in the lateral direction (ie within the plane of the film) are forced to match the lattice parameters of the substrate
- This distorts the unit cell of the film
A formerly cubic unit cell is now tetragonal

Application of Diffraction Data

Relaxation and Lattice Strain



- Determine the degree of relaxation
 - No relaxation (fully strained)- the lateral lattice parameters of the film are strained to be identical to the substrate
 - Fully relaxed- the lateral lattice parameters of the film are equal to the bulk values

Application of Diffraction Data

Lattice Strain



The film and substrate may become slightly curved rather than perfectly flat

This may be the result of deposition process, thermal expansion mismatch between the film and substrate, etc

Application of Diffraction Data

Contributions to Microstrain Broadening

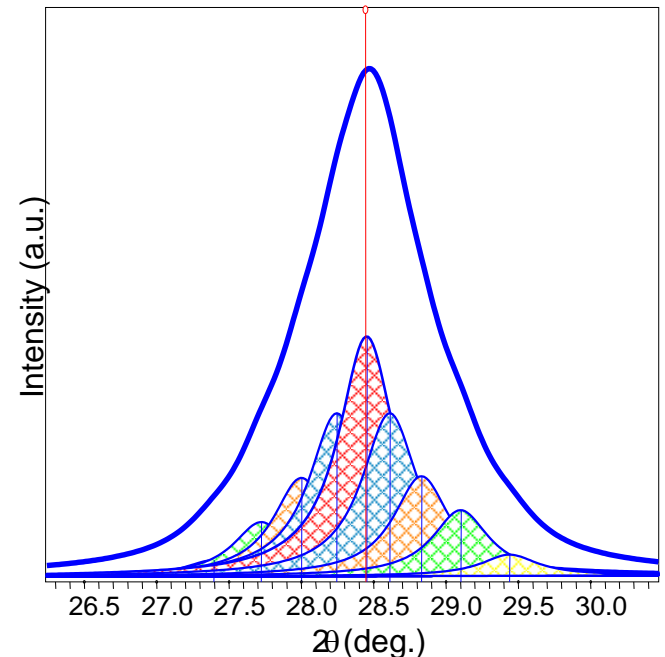
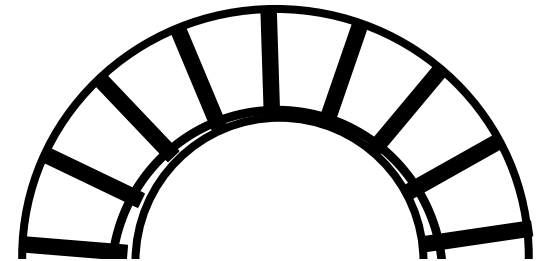
- Non-uniform Lattice Distortions
- Dislocations
- Antiphase Domain Boundaries
- Grain Surface Relaxation

- Other contributions to broadening
 - faulting
 - solid solution inhomogeneity
 - temperature factors

Application of Diffraction Data

Non-Uniform Lattice Distortions

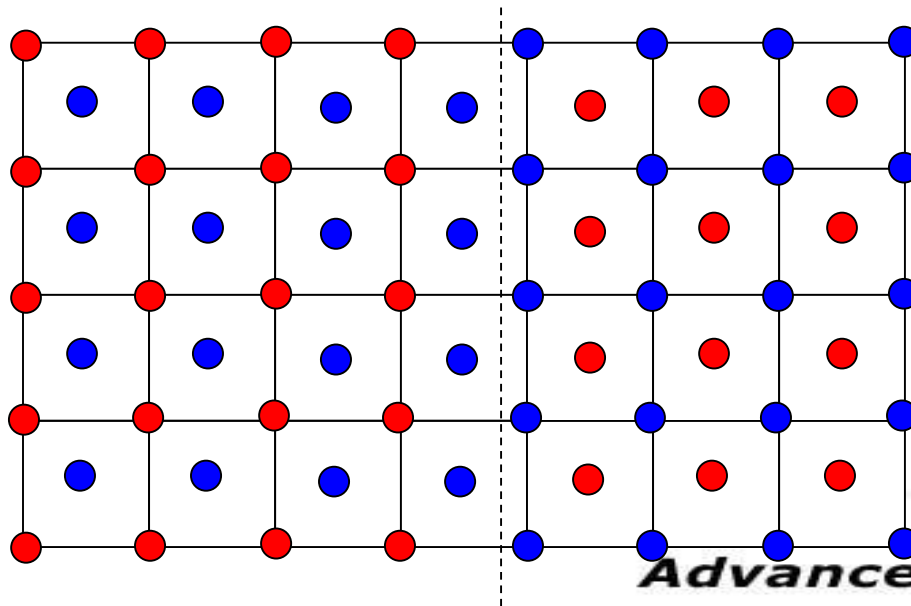
- Rather than a single d-spacing, the crystallographic plane has a distribution of d-spaces
- This produces a broader observed diffraction peak
- Such distortions can be introduced by:
 - surface tension of nanocrystals
 - morphology of crystal shape, such as nanotubes
 - interstitial impurities



Application of Diffraction Data

Antiphase Domain Boundaries

- Formed during the ordering of a material that goes through an order-disorder transformation
- The fundamental peaks are not affected
- the superstructure peaks are broadened
 - the broadening of superstructure peaks varies with hkl



Application of Diffraction Data

Dislocations

- Line broadening due to dislocations has a strong hkl dependence
- The profile is Lorentzian
- Can try to analyze by separating the Lorentzian and Gaussian components of the peak profile
- Can also determine using the Warren-Averbach method
 - measure several orders of a peak
 - 001, 002, 003, 004, ...
 - 110, 220, 330, 440, ...
 - The Fourier coefficient of the sample broadening will contain
 - an order independent term due to size broadening
 - an order dependent term due to strain

Application of Diffraction Data

Faulting

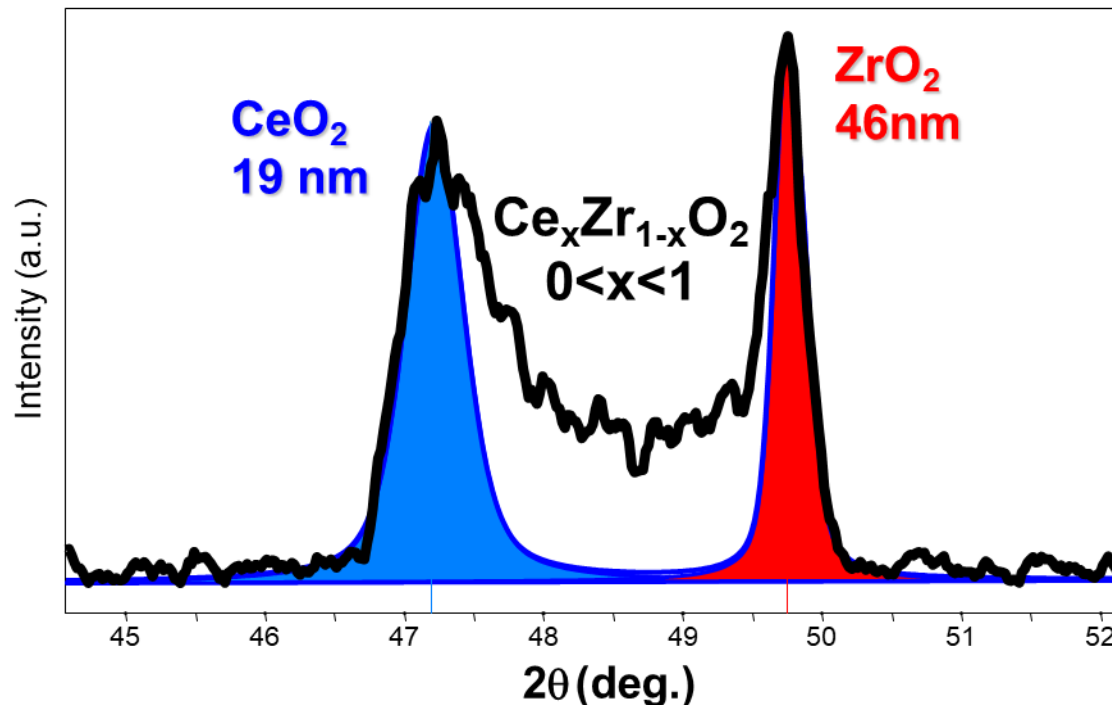
- Broadening due to deformation faulting and twin faulting will convolute with the particle size Fourier coefficient
 - The particle size coefficient determined by Warren-Averbach analysis actually contains contributions from the crystallite size and faulting
 - the fault contribution is hkl dependent, while the size contribution should be hkl independent (assuming isotropic crystallite shape)
 - the faulting contribution varies as a function of hkl dependent on the crystal structure of the material (fcc vs bcc vs hcp)

See Warren, 1969, for methods to separate the contributions from deformation and twin faulting

Application of Diffraction Data

Solid Solution Inhomogeneity

- Variation in the composition of a solid solution can create a distribution of d-spacing for a crystallographic plane
 - Similar to the d-spacing distribution created from microstrain due to non-uniform lattice distortions



Application of Diffraction Data

Temperature Factor

- The Debye-Waller temperature factor describes the oscillation of an atom around its average position in the crystal structure
- The thermal agitation results in intensity from the peak maxima being redistributed into the peak tails
 - it does not broaden the FWHM of the diffraction peak, but it does broaden the integral breadth of the diffraction peak
- The temperature factor increases with 2θ
- The temperature factor must be convoluted with the structure factor for each peak
 - different atoms in the crystal may have different temperature factors
 - each peak contains a different contribution from the atoms in the crystal

$$F = f \exp(-M) \qquad M = 2\pi^2 \left(\frac{\Delta X / \sqrt{3}}{d} \right)^2$$

Application of Diffraction Data

Microstrain Broadening

- lattice strains from displacements of the unit cells about their normal positions
- often produced by dislocations, domain boundaries, surfaces etc.
- strains are very common in nanocrystalline materials
- the peak broadening due to strain will vary as:

$$B(2\theta) = 4\varepsilon \frac{\sin \theta}{\cos \theta}$$

compare to peak broadening due to crystallite size: $B(2\theta) = \frac{K\lambda}{L \cos \theta}$

Application of Diffraction Data

Microstrain Broadening

Analyzing the peak widths over a range of 2θ using a Williamson-Hall plot can let you separate microstrain and crystallite size.

Broadening of a diffraction line due to stress represented by:

$$\beta_{\varepsilon} = 4\varepsilon \tan\theta$$

where,

ε – residual strain (also represented as η)

β_{ε} – (radians) – broadening of observed diffraction peak.

Application of Diffraction Data

Broadening Effects

Since broadening by stress follows a $\tan\theta$ function and broadening by crystallite size has a $1/\cos\theta$ dependence, both effects can be separated out during analysis.

Contributions can be separated if the peaks are Lorentzian or Gaussian-shaped.

Application of Diffraction Data

Williamson-Hall Plot

Dealing With Different Integral Breadth/FWHM Contributions

-Lorentzian and Gaussian Peak shapes are treated differently

-B=FWHM or β in these equations

-Williamson-Hall plots are constructed for both the Lorentzian and Gaussian peak widths.

-The crystallite size is extracted from the Lorentzian W-H plot and the strain is taken to be a combination of the Lorentzian and Gaussian strain terms.

Lorentzian (Cauchy)

$$B_{Exp} = B_{Size} + B_{Strain} + B_{Inst}$$
$$(B_{Exp} - B_{Inst}) = B_{Size} + B_{Strain}$$

Gaussian

$$B_{Exp}^2 = B_{Size}^2 + B_{Strain}^2 + B_{Inst}^2$$
$$(B_{Exp}^2 - B_{Inst}^2) = B_{Size}^2 + B_{Strain}^2$$

Integral Breadth (PV)

$$\beta_{Exp}^2 = \beta_{Lorentzian} \beta_{Exp} + \beta_{Gaussian}$$

If not sure

$$B_{Size} + B_{Strain} = (B_{Exp} - B_{Inst})(B_{Exp}^2 - B_{Inst}^2)$$

Application of Diffraction Data

Broadening Effects

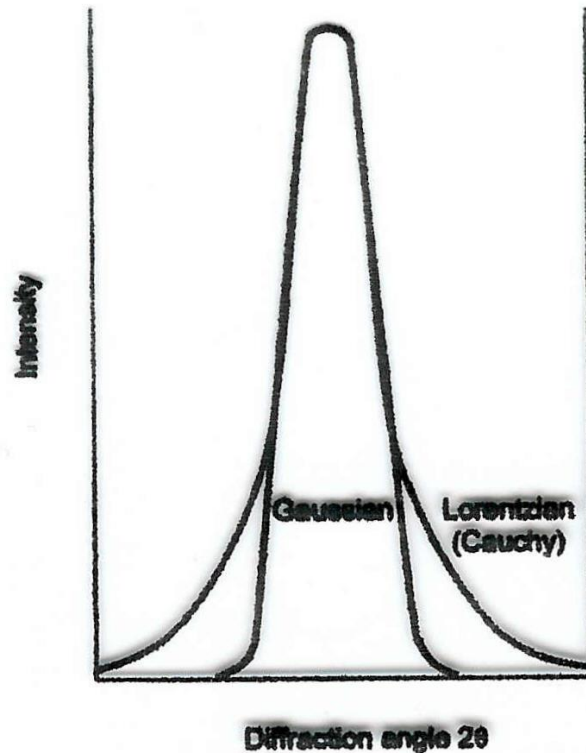


FIG. 6.2. Comparison of symmetrical Lorentzian (Cauchy) and Gaussian x-ray diffraction peak profiles.

Application of Diffraction Data

Broadening Effects

For Lorentzian peaks:

$$\beta_{\text{exp}} = \beta_{\text{size}} + \beta_{\text{strain}} + \beta_{\text{inst}}$$

For Gaussian peaks:

$$\beta_{\text{exp}}^2 = \beta_{\text{size}}^2 + \beta_{\text{strain}}^2 + \beta_{\text{inst}}^2$$

Plot $\beta \cos \theta$ versus $\sin \theta$ (Williamson-Hall Plot)

Application of Diffraction Data

Williamson-Hall Plot

Plot $\beta \cos \theta$ versus $\sin \theta$ (Williamson-Hall Plot)

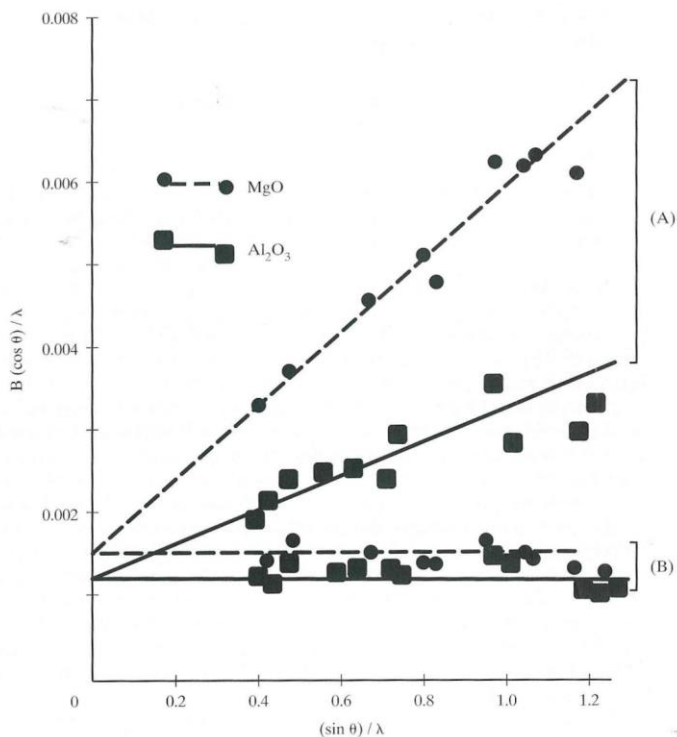


Figure 14-8 Williamson-Hall plot for MgO and Al₂O₃, curves (A) ball milled for 2 hours and (B) ball milled for 2 hours, then annealed for 2 hours at 1350°C. After Lewis and Lindley [14.10].

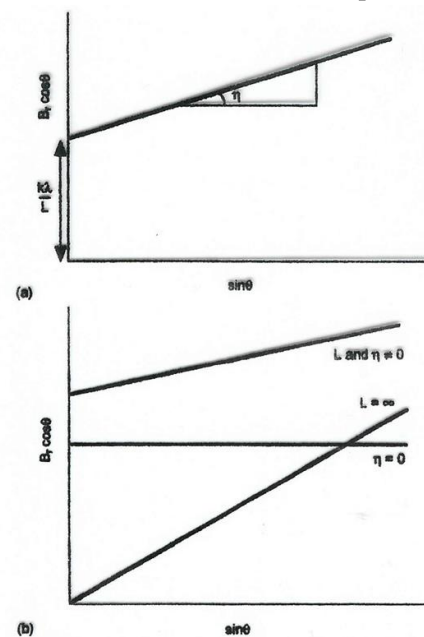


FIG. 6.4. (a) Plot of $B \cos \theta$ against $\sin \theta$, indicating that the intercept (λ/L) and slope (η) can be used to calculate the crystallite size (L) and lattice strain (η), respectively. (b) Typical plots to show the relative positions of the straight line for very large crystallite sizes ($L = \infty$), no strain ($\eta = 0$), and when both lattice strain and crystallite size contribute to peak broadening.

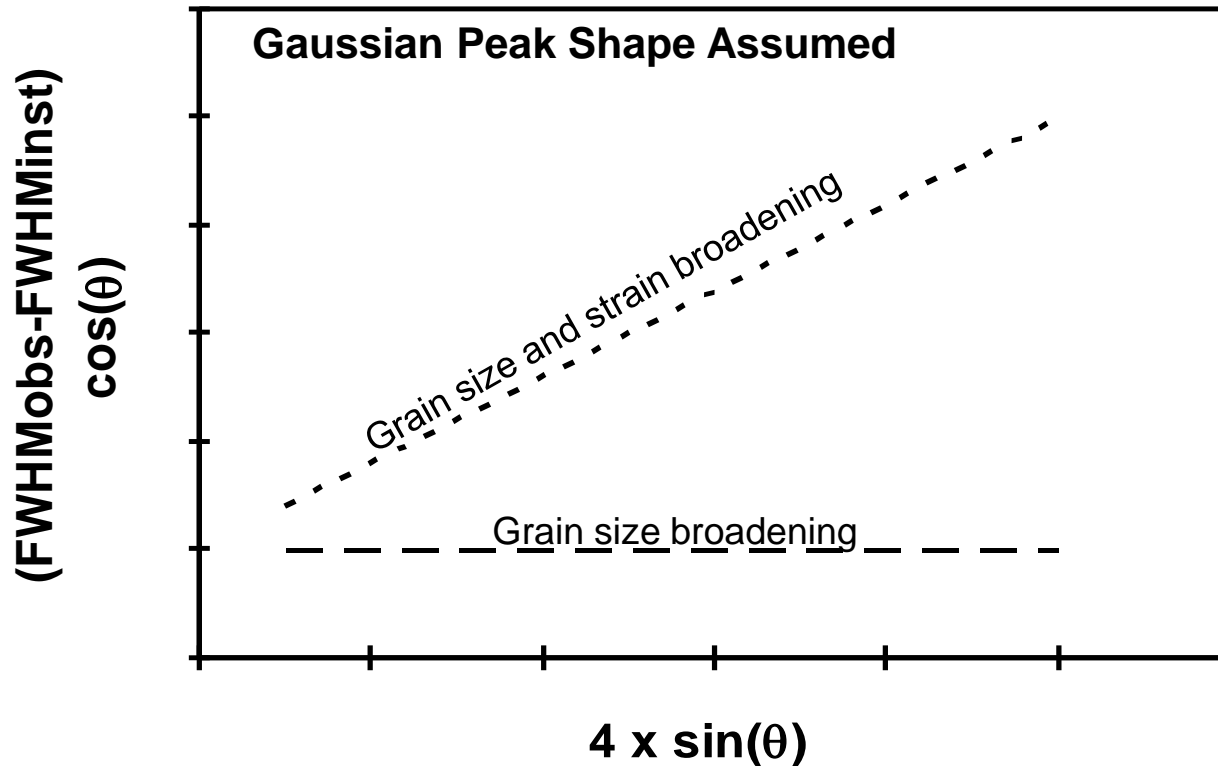
Application of Diffraction Data

Williamson-Hall Plot

y-intercept

slope

$$FWHM \times \cos(\theta) = \frac{K \times \lambda}{Size} + Strain \times 4 \times \sin(\theta)$$



Application of Diffraction Data

Broadening Effects – Ex: CeO₂

Contributions of crystallite size and strain are given by the following equation:

$$\beta_r \cos \theta = \frac{k\lambda}{L} + \eta \sin \theta$$

where

λ is the wavelength of the x-rays,

θ is the diffraction angle,

η is the strain,

L is the crystallite size,

k is a constant (0.94 for gaussian line profiles and small cubic crystals of uniform size)

β_r is the corrected full width at half maximum of the peak

Application of Diffraction Data

Broadening Effects

β_r is the corrected full width at half maximum of the peak given by,

$$\beta_r^2 = \beta_m^2 - \beta_s^2$$

where

β_m is the experimental measured half width

β_s is half width of a silicon powder standard with peaks corresponding to the same 2θ region.

Application of Diffraction Data

Broadening Effects Williamson-Hall Plot

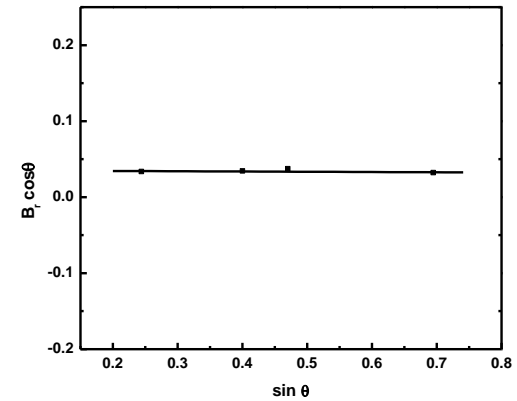
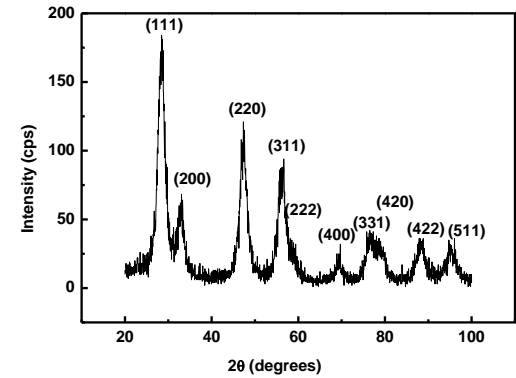
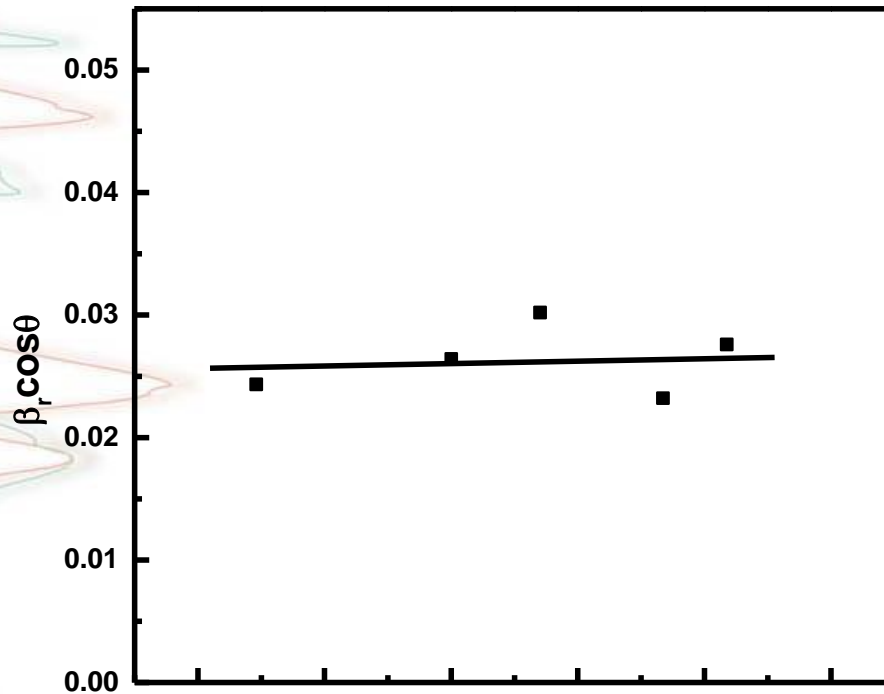


Figure 4. (a) X-ray diffraction pattern of CeO_2 powder produced from a solution of 0.1 M $\text{Ce}(\text{NO}_3)_3$ and 0.5 M acetate at pH ~ 11 at applied potential of 1.10V vs SCE. The synthesis was operated at room temperature. (b) Williamson-Hall plot $\beta_r \cos\theta$ versus $\sin\theta$ for the XRD pattern for (a).

Application of Diffraction Data

Other Methods

Most alternative XRD crystallite size analyses use the Fourier transform of the diffraction pattern

- **Variance Method**
 - Warren Averbach analysis- Fourier transform of raw data
 - Convolution Profile Fitting Method- Fourier transform of Voigt profile function
- **Whole Pattern Fitting in Fourier Space**
 - Whole Powder Pattern Modeling- Matteo Leoni and Paolo Scardi
 - Directly model all of the contributions to the diffraction pattern
 - each peak is synthesized in reciprocal space from its Fourier transform
 - for any broadening source, the corresponding Fourier transform can be calculated

Application of Diffraction Data

Other Methods

Most alternative XRD crystallite size analyses use the Fourier transform of the diffraction pattern

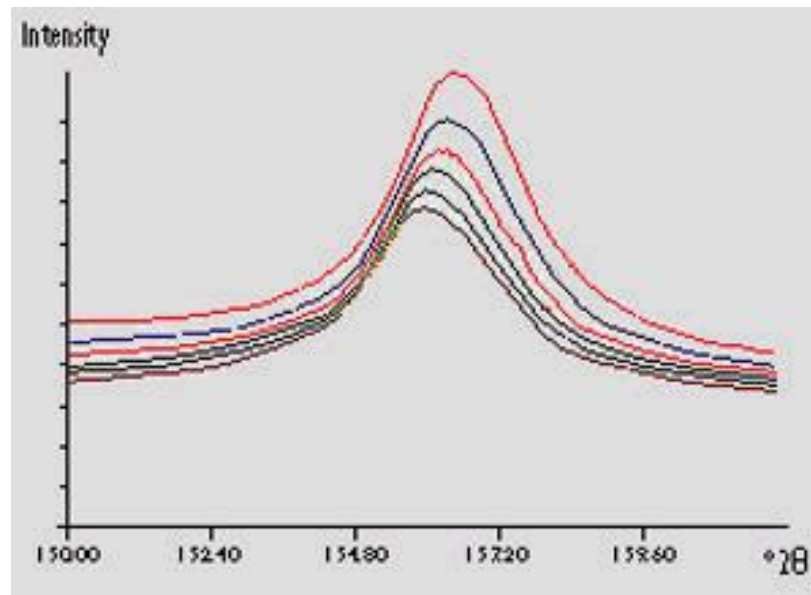
- **Fundamental Parameters Profile Fitting**
 - combine with profile fitting, variance, or whole pattern fitting techniques
 - instead of deconvoluting empirically determined instrumental profile, use fundamental parameters to calculate instrumental and specimen profiles

Application of Diffraction Data

Other Methods

Stress Analysis

Stress is determined by recording the angular shift of a given Bragg reflection as a function of sample tilt (psi). This actually provides a measure of strain in the sample from which the stress can then be calculated by plotting the change in d-spacing against $\sin^2\psi$.



Application of Diffraction Data

Example – Golden Lab - Cerium Oxide

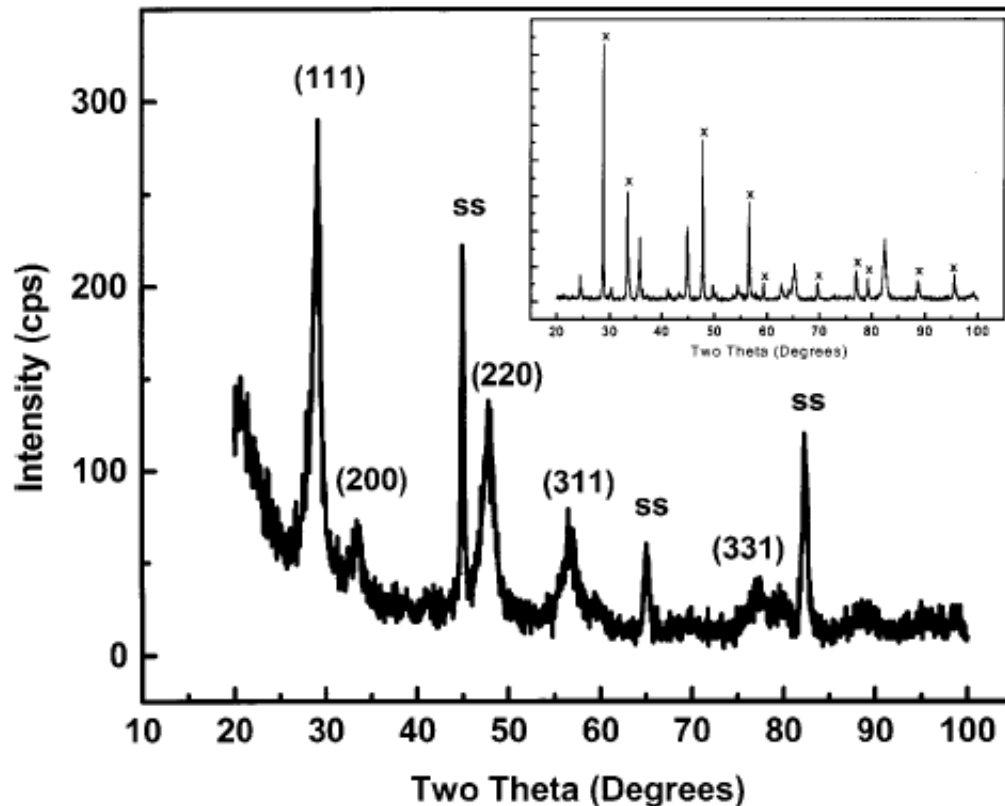


FIG. 1. XRD pattern for a nanostructured CeO₂ film electrodeposited on a stainless-steel substrate. Inset: Electrodeposited cerium oxide film sintered at 900 °C for 5 h. x—CeO₂ reflections for the fluorite structure.

Application of Diffraction Data

Example – Golden Lab - Cerium Oxide

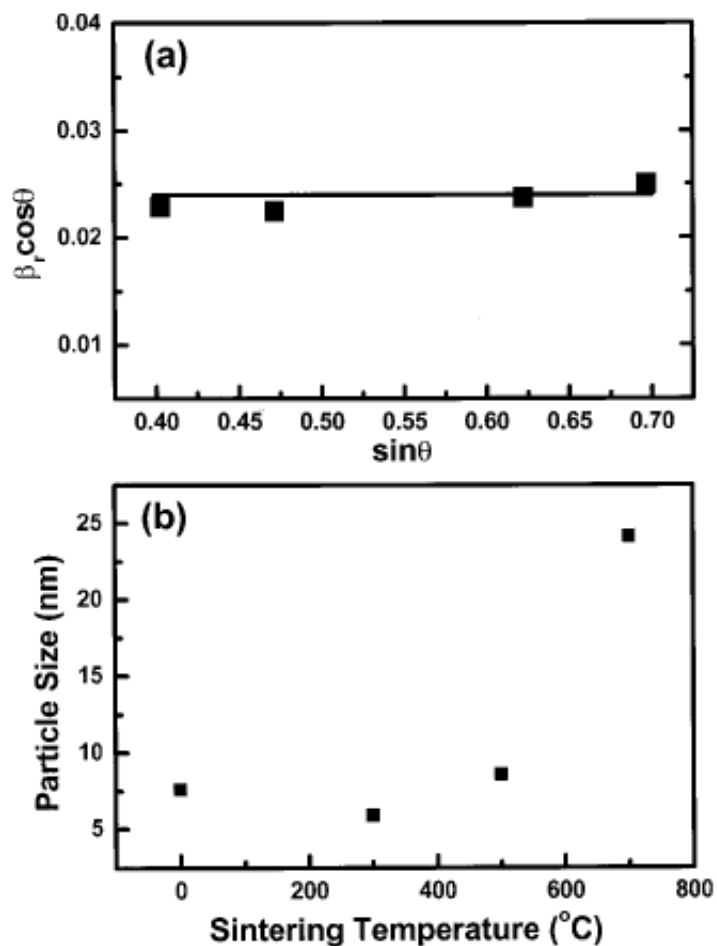


FIG. 2. (a) Williamson-Hall plot of $\beta \cos \theta$ vs $\sin \theta$ for the XRD pattern from Fig. 1. (b) Crystallite size vs sintering temperature calculated from XRD data of electrodeposited CeO_2 films.

Application of Diffraction Data

Example – Golden Lab – NiLDH

Table 3 Strain and particle size of each sample as determined from Williamson–Hall analysis of the X-ray diffraction data

Sample	Strain (η)	Particle size (nm)
A1	0.0083	16.09
B1	0.0043	19.05
B2	0.0175	34.48

$$B_r^2 = B_0^2 - B_i^2$$

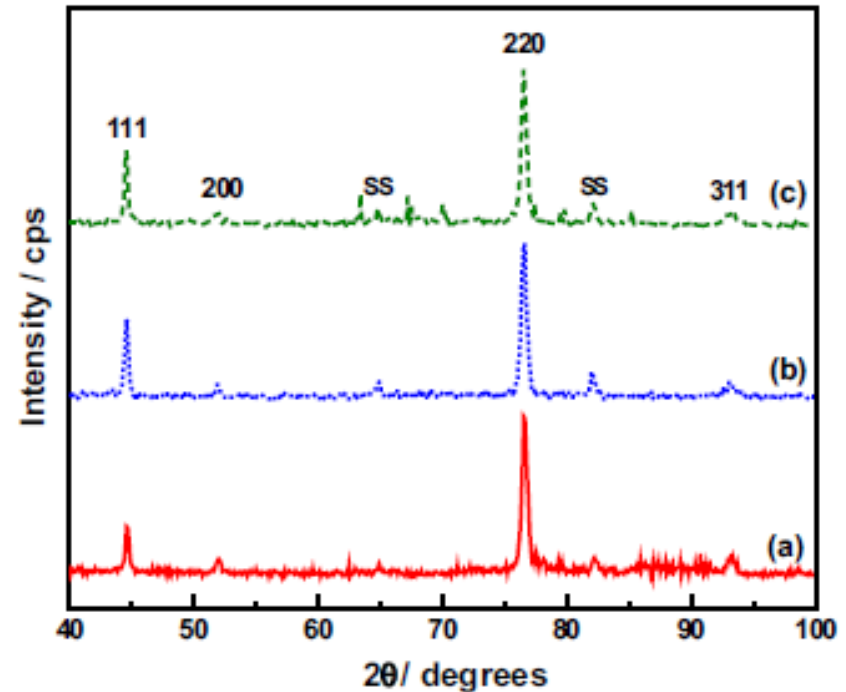


Fig. 2 X-ray diffraction patterns of each nickel coating *a* A1 (solid line), *b* B1 (dotted line), and *c* B2 (dashed line)

Application of Diffraction Data

Example – Golden Lab – Ni and NiOH

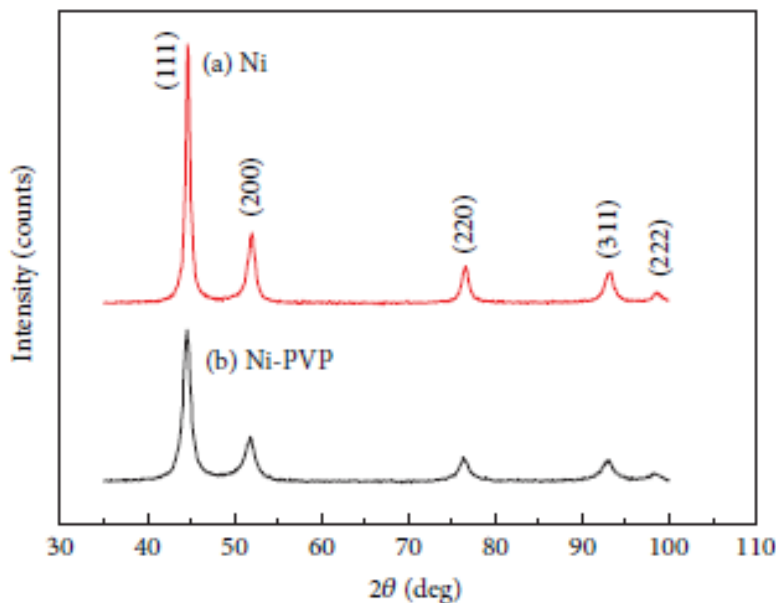


FIGURE 1: XRD pattern of (a) nickel and (b) nickel powders stabilized by PVP, precipitated by a chemical reduction method and sonication at temperature 55–65°C.

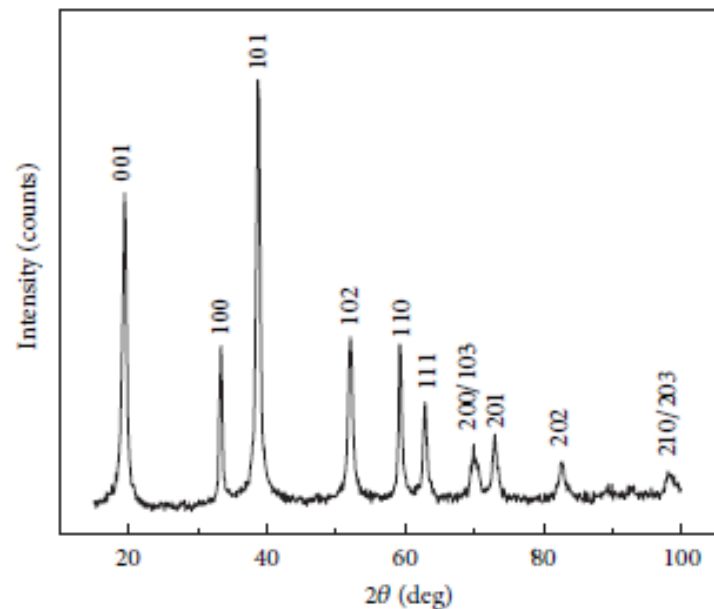


FIGURE 3: XRD pattern of precipitated nickel hydroxide powder produced by titrating nickel chloride with hydrazine-sodium hydroxide solution at pH ~10.

Application of Diffraction Data

Example – Golden Lab – Ni and NiOH

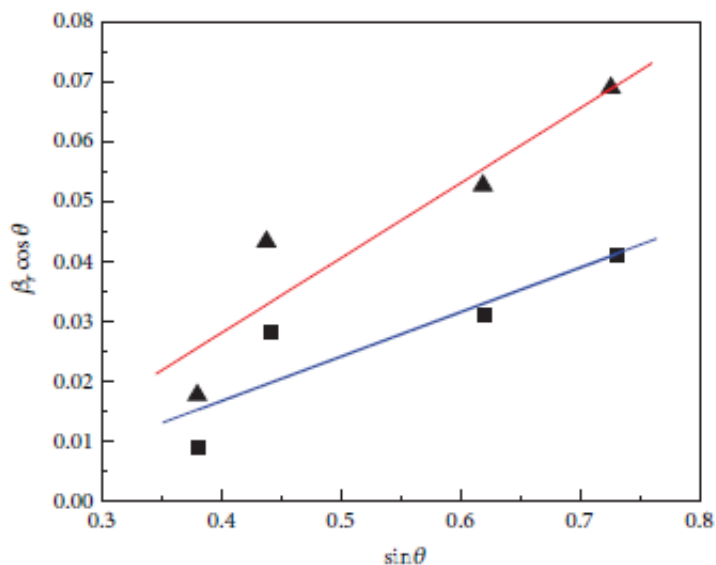


FIGURE 2: Williamson-Hall plot for XRD data of nickel powder (squares, blue line fit) and PVP-protected nickel particles (triangles, red fit lines).

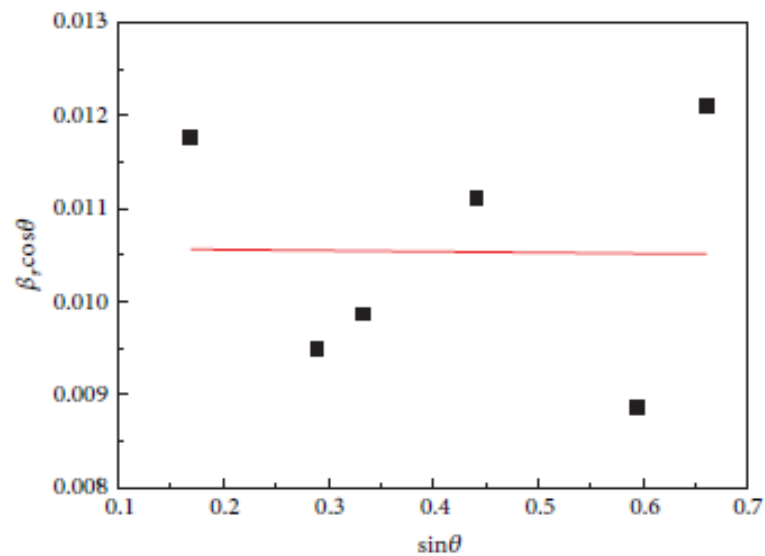


FIGURE 4: Williamson-Hall plot for XRD data of Ni(OH)₂ synthesized powder.

TABLE 1: Particle size of the nanopowders measured using the Williamson-Hall analysis from the X-ray diffraction data and the dynamic light scattering method.

Nanopowders	Measured particle size (nm)	
	Williamson-Hall plot	Dynamic light scattering ($n = 40$)
Nickel	12	101.7 ± 25.6
Nickel-PVP	7	25.9 ± 4.4
Nickel hydroxide	14	63.1 ± 16.2

Homework Assignment: Precise Lattice Parameters

Due 12-3-24

Homework Assignment: Determination Crystallite Size and Lattice Strain
Due 12-5-24

Final – Dec 10th 8 am to 10 am